Application of Equation of State Theories to Narrow Molecular Weight Distribution Mixtures of Polystyrene and Poly(vinyl methyl ether)

D. J. Walsh* and G. T. Dee

Central Research and Development Department, E. I. du Pont de Nemours and Company, Inc., Experimental Station, Wilmington, Delaware 19898

J. L. Halary, J. M. Ubiche, M. Millequant, J. Lesec, and L. Monnerie

Unite Associee au C.N.R.S. No. 278, E.S.P.C.I., 10 rue Vauquelin, 75231 Paris Cedex 05, France. *Received August 17, 1988; Revised Manuscript Received January 24, 1989*

ABSTRACT: A comparison has been made of the equation of state theories of Flory, Orwoll, and Vrij (FOV) and the cell model for describing the miscibility and phase behavior of polystyrene/poly(vinyl methyl ether) mixtures. Phase diagram determinations were performed on samples of narrow molecular weight distribution in order to reduce polydispersity effects. *PVT* data were used to obtain the reduction parameters of the pure components. From these the phase diagrams of the blends were simulated by using the theories. The FOV equation gives a predicted phase diagram that is qualitatively at variance with experiment since it predicts the minimum in the phase diagram to occur at much higher polystyrene volume fractions. The cell model is closer to experiment in this respect.

Introduction

A necessary but not sufficient criterion for miscibility to occur is that the free energy of mixing be negative. A precise requirement is that its second differential with respect to composition be positive over the entire composition range. The free energy of mixing can be considered as arising from three contributions, the combinatorial entropy, an interactional term that is usually specified by an interaction parameter, and a contribution from free-volume changes on mixing. The last of these is often included within the interaction term, but this is not satisfactory for a realistic description of polymer mixtures.

Various theories have been developed that attempt to describe the effect of volume changes on polymers, polymer solutions, and mixtures. Well-known theories are those attributed to Simha and Somcynsky,[1] Sanchez and Lacombe,[2] and Flory and co-workers,[3,4] and of these the last has been most extensively applied. In a recent publication we showed that a simple cell model provided a tractable and analytically simple equation of state that described the *PVT* properties of polymer melts more accurately than did the theory of Flory and co-workers.[5] We also have shown that a semiempirical modification of this equation produced a modified cell model that described the data even better, approaching the accuracy of the data.[6]

In this paper we describe a comparison of the application of the equation of Flory and co-workers (FOV) and the cell model (CM) to polymer mixtures. The system that has been studied is polystyrene/poly(methyl vinyl ether) (PS/PVME) blends. Reported results show that PS and PVME are miscible at room temperature and phase separate on heating in the 100–200 °C region.[7-11] The phase diagram has been shown to be very sensitive to molecular weight,[7-11] to deuteration of one component,[12-14] and also to polydispersity.[14]

Unfortunately, all the data available in the literature deal with markedly polydisperse PVME. As a consequence, they may yield experimental diagrams at variance with theoretical calculations based on binary polymer mixtures.[15] To overcome this obstacle, we consider here new phase-separation data for different blends of PS/PVME mixtures containing fractionated PVME samples.

Experimental Section

Materials. The molecular weight characteristics of the polymers used for the determination of the phase diagrams are given in Table I. The polystyrenes are commercially available materials (PS35, 67-Polymer Labs, PS106-Pressure Chem., PS233-Polysciences) with very narrow chain-length distribution (M_w/M_n = 1.06). The PVME samples were fractionated by preparative gel permeation chromatography from 2% methylene chloride solutions of commercial PVME (M_w = 99 000 g/mol, M_w/M_n = 2.12; Scientific Polymer Products). Fractionation was performed on a Waters column (length 150 cm, i.d. 2.7 cm) filled with Microstyragel (mixture of commercial beads of 10^2, 10^3, 10^4, and 10^5 nm). Five fractions were isolated from the original material. Each fraction was then refractionated in the same column to make it free from the aisles of the distribution and reduce its polydispersity.

Table I
Characteristics of the Polymers Used for the Determination of the Phase Diagrams

sample	wt av mol wt M_w, g/mol	no. av mol wt M_n, g/mol	polydispersity M_w/M_n
PS 233	233 000	220 000	1.06
PS 106	106 000	100 000	1.06
PS 67	67 000	62 000	1.08
PS 35	35 700	34 000	1.05
PVME 152	152 000	135 000	1.13
PVME 95	95 000	75 000	1.27
PVME 77	77 000	62 000	1.24
PVME 56	56 000	38 000	1.47
PVME 45	45 000	22 000	2.05

Phase Diagram Determination. Phase diagrams were determined on 100-μm-thick films by using the fluorescence emission technique used in previous studies[10,11,13,14] and presented in detail in ref 16. Films of PS/PVME mixtures were cast at room temperature from 10% benzene solutions containing also a few labeled PS chains (which include a dimethylanthracene group in their middle). After solvent removal, the label content of the films was around 6 ppm of anthracene units. Fluorescence emission measurements were carried out under a fluorescence microscope, which is especially useful in the case of very small samples. The immiscibility threshold was detected in the form of an upturn in fluorescence intensity, observed either under continuous heating at a rate of 0.2 °C/min or, with increased accuracy, under isothermal conditions. The results for isothermal conditions are less by 2 or 3 °C depending on polymer molecular weight.

The experimental phase diagrams for PVME 95 with PSs of different molecular weights and for PS 106 with different PVMEs of narrow molecular weight distribution are given in Figures 1a and 2a, respectively. From a qualitative viewpoint, these diagrams do not differ markedly from those observed by using either commercial PVME or the polydisperse sample PVME 45.[10] A careful inspection of the data shows that both temperature and

0024-9297/89/2222-3395$01.50/0

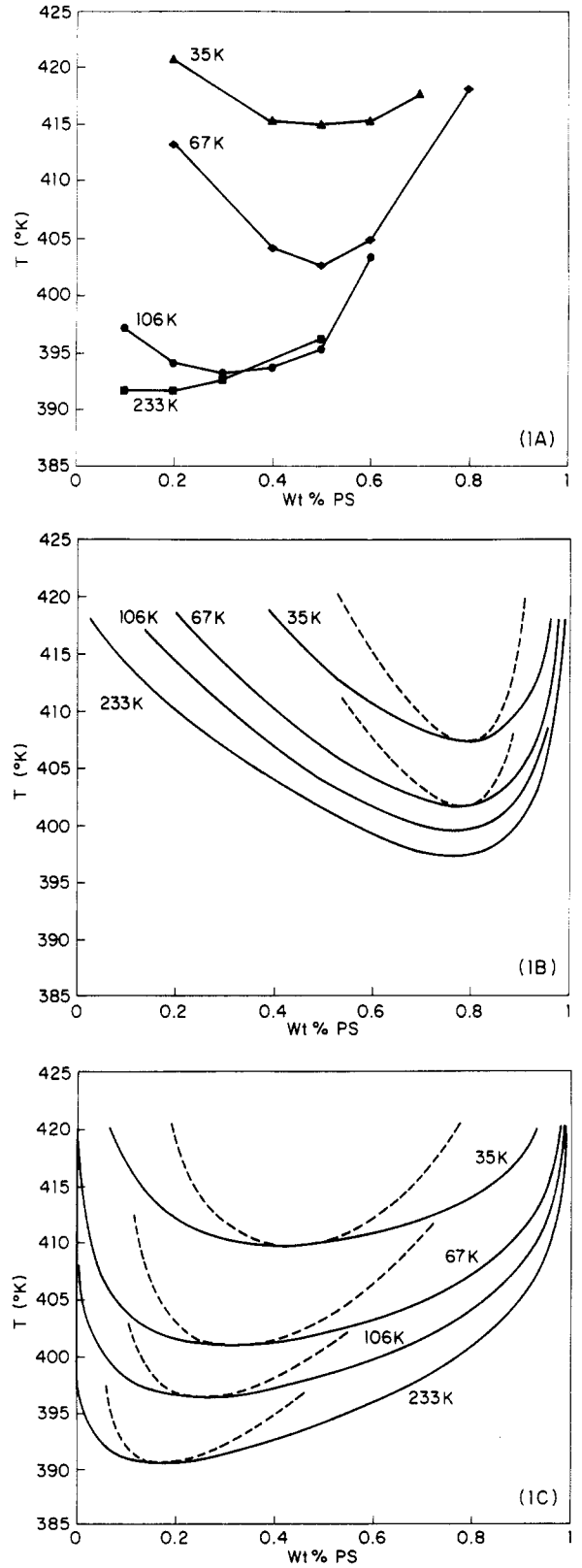

Figure 1. Phase diagrams for PVME (M_w 95 000) with PS of different molecular weights: 1A show the experimental results; 1B shows binodals (solid lines) and spinodals (dashed lines) calculated by using the FOV equation of state; 1C shows binodals and spinodals calculated by using the cell model.

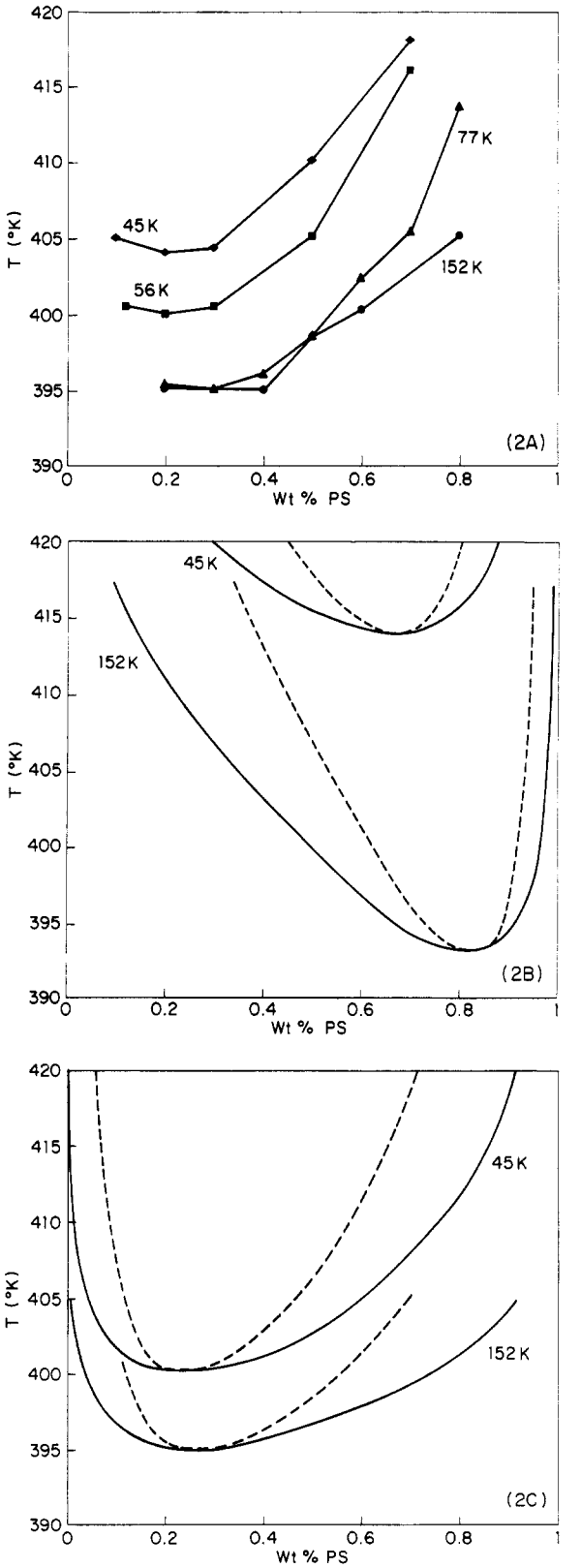

Figure 2. Phase diagrams for PS (M_w 106 000) with PVME of different molecular weights: 2A shows the experimental results; 2B shows the binodals (solid lines) and spinodals (dashed lines) calculated by using the FOV equation to state (only two shown for clarity); 2C shows the binodals and spinodals calculated by using the cell model.

composition of the minimum of the phase boundary depend on polydispersity. Such an analysis is not the purpose of the present paper, and it will be discussed in a forthcoming publication.

Theory

We describe the basic formalism for a mixture of two components. We consider the two models within the context of the cell model formalism.[17,18] The FOV model differs from the cell model in that a van der Waals potential is used to describe the attractive interaction between the mers in the system. The other model employs a Lennard-Jones 6–12 interaction potential.

Consider a mixture containing N_1 molecules of the first component and N_2 molecules of the second. The two components are characterized by their reduction parameters P^*_i, V^*_i, and T^*_i, where $i = 1, 2$. If $N = N_1 + N_2$ is the total number of molecules in the system, r_1 and r_2 are the number of mers per molecule of the respective components, c_1 and c_2 are the number of effective degrees of freedom per mer for each component, and s_1 and s_2 are the number of nearest-neighbor contacts of the mers of the respective components, then we define the following quantities:

$$x_1 \equiv N_1/N = 1 - x_2 \tag{1}$$

$$r \equiv x_1 r_1 + x_2 r_2 \tag{2}$$

$$\phi_1 \equiv r_1 N_1/rN = 1 - \phi_2 \tag{3}$$

$$s \equiv \phi_1 s_1 + \phi_2 s_2 \tag{4}$$

$$c \equiv \phi_1 c_1 + \phi_2 c_2 \tag{5}$$

With these definitions we define the following rules which we will use for the mixture.

(a) The hard-core mer volumes are defined to be equal:

$$v^*_1 = v^*_2 = v^* \tag{6}$$

(b) The hard-core volume of the mixture, V^*, is equal to the sum of the hard-core volumes of the components:

$$V^* = rNv^* \tag{7}$$

(c) The number of pair interactions in the mixture is equal to the sum of the pure-component pair interactions, i.e., if N_{ij} is the number of i,j pair interactions, then

$$N_{11} + N_{12} + N_{22} = \tfrac{1}{2}(s_1 r_1 N_1 + s_2 r_2 N_2) = srN/2 \tag{8}$$

With the above definitions and rules, the partition function for the mixture can be written in the following form:

$$Z(V,T) = Z_{\text{int}}(T) Z_{\text{comb}} (v^{1/3} - \gamma v^{*1/3})^{3(c_1 r_1 N_1 + c_2 r_2 N_2)} \exp(-E_0/kT) \tag{9}$$

where $Z_{\text{int}}(T)$ is the contribution from the motion of the mers within their respective cells, and Z_{comb} is the Flory–Huggins combinational entropy, which is of the form such that

$$\ln Z_{\text{comb}} = N_1 \ln \phi_1 + N_2 \ln \phi_2 \tag{10}$$

The third factor is the so-called "free volume" term where the cell potential has been approximated by a square-well potential. The factor γ is a geometrical factor associated with the cell geometry used and v is the cell volume. The function $E_0(V)$ is the interaction energy computed when all mers are at their cell centers, and for mixtures it is of the form

$$-E_0(V) = (N_{11}\eta_{11} + N_{12}\eta_{12} + N_{22}\eta_{22})\psi(v) \tag{11}$$

where η_{ij} is the characteristic energy of interaction between mers of component i and j and $\psi(v)$ is the interaction potential. For the FOV, $\psi(v)$ is of the form

$$\psi(\tilde{v}) = -2v^*/v \equiv -2/\tilde{v} \tag{12}$$

For the cell models $\psi(v)$ is the 6-12 Lennard-Jones potential:

$$\psi(\tilde{v}) = -4\left(\frac{2A}{\tilde{v}^2} - \frac{B}{\tilde{v}^4}\right) \tag{13}$$

where A and B are geometrical factors. If random mixing of the two mers is assumed, then

$$N_{11} = \tfrac{1}{2}(s_1 r_1 N_1 \Theta_1), \quad N_{22} = \tfrac{1}{2}(s_2 r_2 N_2 \Theta_2), \quad N_{12} = s_1 r_1 N_1 \Theta_2 \tag{14}$$

where $\Theta_1 = s_1 r_1 N_1/srN = 1 - \Theta_2$. Using these definitions, we can write

$$-E_0/rN = \tfrac{1}{2}(\Theta_1\epsilon_1 + \Theta_2\epsilon_2 - s_1\Theta_1\Theta_2\Delta\eta) \tag{15}$$

where $\Delta\eta = \eta_{11} + \eta_{22} - 2\eta_{12}$ and $\epsilon_i = s_i\eta_{ii}$. If we define an interaction parameter X_{12} so that

$$X_{12} \equiv s_1\Delta\eta/v^* \tag{16}$$

then eq 11 becomes

$$-E_0/rN = 2(\epsilon_1\phi_1 + \epsilon_2\phi_2 - v^*X_{12}\phi_1\Theta_2)\psi(\tilde{v}) \equiv 2\epsilon\psi(\tilde{v}) \tag{17}$$

Since P^* and T^* are defined as

$$P^* = \epsilon/v^* \qquad T^* = \epsilon/ck$$

eq 17 leads to a definition of P^* and T^* for the mixtures of the form

$$P^* = \phi_1 P^*_1 + \phi_2 P^*_2 - X_{12}\phi_1\Theta_2 \tag{18}$$

$$T^* = \frac{P^*}{\phi_1(P^*_1/T^*_1) + \phi_2(P^*_2/T^*_2)} \tag{19}$$

Finally, if we define $\tilde{P} = P/P^*$ and $\tilde{T} = T/T^*$, the partition function can be written in the form

$$Z(v,T) = \alpha v^{*crN} Z_{\text{comb}} (\tilde{v}^{1/3} - \gamma)^{3crN} \exp(2crN\psi(\tilde{v})/\tilde{T}) \tag{20}$$

where we have neglected the temperature dependence resulting from the motion of the mers within the cells. The effects of this contribution will be studied at a later date.

Using (20), we can then compute the chemical potential using the expression

$$\Delta\mu_1 = kT\left(\left.\frac{\partial(\ln Z)}{\partial N_1}\right|_{T,V,N_2} - \left.\frac{\partial(\ln Z)}{\partial N_1}\right|_{T,V,N_2=0}\right) \tag{21}$$

$$= kT\left[\ln\phi_1 + \phi_2\left(1 - \frac{r_1}{r_2}\right)\right] + r_1\epsilon_1\left[3\tilde{T}\ln\left(\frac{\tilde{v}_1^{1/3} - \gamma}{\tilde{v}^{1/3} - \gamma}\right) + \tilde{P}_1(\tilde{v} - \tilde{v}_1)\right] + F(\tilde{v}) \tag{22a}$$

where

$$F(\tilde{v}) = r_1\epsilon_1\left(\frac{1}{\tilde{v}_1} - \frac{1}{\tilde{v}}\right) + \frac{r_1 v^*}{\tilde{v}} X_{12}\Theta_2^2 \tag{22b}$$

for the FOV equation and

$$F(\tilde{v}) = r_1\epsilon_1\left[A\left(\frac{1}{\tilde{v}_1^2} - \frac{1}{\tilde{v}^2}\right) - \frac{B}{2}\left(\frac{1}{\tilde{v}_1^4} - \frac{1}{\tilde{v}^4}\right)\right] + r_1 v^* X_{12}\Theta_2^2\left(\frac{A}{\tilde{v}^2} - \frac{B}{2\tilde{v}^4}\right) \tag{22c}$$

for the cell model. For a hexagonal close packed geometry $A = 1.2045$ and $B = 1.011$. For the FOV model $\gamma = 1$ and for the cell model $\gamma = 0.8909$.

Using (22) and a similar expression for $\Delta\mu_2$, we can compute $\Delta\mu_1$ and $\Delta\mu_2$ and locate the phase diagram for this binary system by seeking solutions to the equations

$$\Delta\mu_1^{\text{I}} = \Delta\mu_1^{\text{I}} \tag{23a}$$

$$\Delta\mu_2^{\text{II}} = \Delta\mu_2^{\text{II}} \tag{23b}$$

Table II
State Parameters for PS and PVME for Two Equations of State and Goodness of Fit (See Text)

	P^*, MPa		V^*, cm^3/g		T^*, K		S^2, MPa^2	
	PS	PVME	PS	PVME	PS	PVME	PS	PVME
FOV	489.3	532.3	0.84038	0.833766	8479.9	7163.4	0.43	0.18
CM	608.9	604.3	0.91360	0.908901	4909.4	4172.9	0.5	0.265

where the superscripts I and II indicate two different phases. In practice these solutions, if they exist, are determined numerically.

The spinodals are determined by finding solutions of the equation

$$\left.\frac{d\Delta\mu_1}{d\phi_2}\right|_{\phi_2^s} = \left.\frac{d\Delta\mu_2}{d\phi_2}\right|_{\phi_2^s} = 0 \qquad (24)$$

where ϕ_2^s denotes the value of ϕ_2 at which eq 24 is satisfied. These values are determined numerically for each equation of state.

Results

We modeled the phase diagram using the two equations of state based on the cell model formalism. In all cases we extract the reduction parameters (P^*,v^*,T^*) for the pure components by using PVT data as described in a previous publication.[5] Using the mixture combining rules and eq 23, we search for solutions. If none exist, the polymers are miscible. The application of the combining rules necessitates the introduction of the parameter X_{12}. While an upper bound can be set for this parameter, we adjust it so that the phase diagram is located within the temperature domain where the phase diagram is observed experimentally. Our goal in this present study is to investigate the qualitative details of the phase diagrams as predicted by the models.

The PVT data for both samples were chosen to be in the range 100–200 °C and 10–30 MPa. Table II shows the reduction parameters obtained for PS (M_w = 120000) and PVME (M_w = 74000). The reduction parameters are not expected to be dependent on molecular weight within experimental error for reasonably high values (above 20000).[19]

Also shown is the goodness of fit parameter

$$S^2 \equiv \frac{\sum(P_{data} - P_{fit})^2}{N - 3} \qquad (25)$$

where P_{data} is the measured pressure, P_{fit} is the value predicted by the equation of state, and N is the number of data points. Because of the small block of data, which was chosen to give each equation the best chance to describe the data within the region of interest, the variation in these numbers represents just noise in the data. If larger blocks of data are used, the value of S^2 will increase with the size of the data set and increases fastest for the FOV equation, which is not as good a fitting equation for PVT data as the cell model is,[5] giving values of 10 or more for large data sets.

Figures 1B,C and 2B,C show the phase diagrams as computed for the two different models as functions of PS molecular weight and PVME molecular weight. For the FOV equation, Figures 1B and 2B, the binodal curve occurs at high weight fractions of PS in contradiction to the experimental observations shown in Figures 1A and 2A. The cell model shows the minimum occurring at low weight fractions of PS in agreement with the experimental data. The FOV equation also shows a poor description of the molecular weight dependence of the critical temperature. Both of these facts can be attributed to the relation between the values of P^* for the two polymers. Similar values of P^* for the two polymers will put the phase diagram in the correct composition range. The molecular weight dependence of the phase separation temperature varies with composition (i.e., changing molecular weight moves the phase separation temperature more at compositions richer in one component) and this factor comes close to experimental values as the curve minimum is moved to the correct composition value. The values of P^* for the two polymers from the FOV equation are different from each other well within any experimental uncertainty and for any choice of data block size. It is worth noting that P^* depends on the interaction energy, and it is in the form of potential used that the equations differ. Another factor that can affect the simulation is the value of S_2/S_1, the ratio of surface areas per unit volume, used in the calculation. We have used a value of 1. The phase diagram can be moved by changing this value but not to a large enough extent to change our conclusions for any rational value. The use of a concentration-dependent X_{12} could also change the simulation, but we have no grounds for using any particular values of this dependence.

Another factor that could still be of importance in the details of the shapes of the phase diagram is polydispersity, since the PVME fractions still have appreciable width in molecular weight distribution especially at low molecular weight. The values of X_{12} used to fit the data, −1.78 J/cm^3 for the FOV equation and −1.76 J/cm^3 for the cell model are similar, which may reflect some underlying similarities in the models.

There are other equations of state in the literature that can be used to describe the properties of polymer liquids. The lattice fluid model of Sanchez and Lacombe is perhaps the most well-known of these after the FOV equation. We have applied this equation to this present problem. We fit the equation to the PVT data and determined the relevant reduction parameters. A value of X_{12} = −1.77 was used to adjust the position of the phase diagram at a particular temperature so as to correspond to the experimental observations. We then compared the shape of the calculated phase diagram with experimental results. The calculated phase diagrams exhibited the same character as those calculated by using the FOV equation, namely, the critical composition occurs at high weight fractions of PS in contradiction to the experimental results.

Conclusion

For the polystyrene/poly(vinyl methyl ether) mixtures the FOV equation gives a predicted phase diagram that is qualitatively at variance with experiment since it predicts the minimum in the phase diagram to occur at much higher polystyrene volume fractions. The cell model is closer to experiment in this respect.

Registry No. PS, 9003-53-6; PVME, 9003-09-2.

References and Notes

(1) Somcynsky, T.; Simha, R. *J. Appl. Phys.* **1971**, *42*, 4545.
(2) Sanchez, I. C.; Lacombe, R. H. *J. Phys. Chem.* **1976**, *80*, 2352.
(3) Flory, P. J.; Orwoll, R. A.; Vrij, A. *J. Am. Chem. Soc.* **1964**, *86*, 3567.
(4) Eichinger, B. E.; Flory, P. J. *Trans. Faraday Soc.* **1968**, *65*, 2035.
(5) Dee, G. T.; Walsh, D. J. *Macromolecules* **1988**, *21*, 811.

(6) Dee, G. T.; Walsh, D. J. *Macromolecules* **1988**, *21*, 815.
(7) Bank, M.; Leffingwell; Thies, C. J. *J. Polym. Sci.* **1972**, *A-2*, 1097.
(8) Nishi, T.; Wang, T. T.; Kwei, T. K. *Macromolecules* **1975**, *8*, 227.
(9) Snyder, H. L.; Meakin, P.; Reich, S. *Macromolecules* **1983**, *16*, 757.
(10) Halary, J. L.; Ubrich, J. M.; Nunzi, J. M.; Monnerie, L.; Stein, R. S. *Polymer* **1984**, *25*, 956.
(11) Lennard-Jones, J. E.; Devonshire, A. F. *Proc. R. Soc. (London)* **1937**, *A163*, 53.
(12) Prgogine, I. *The Molecular Theory of Solutions*; North Holland: Amsterdam, 1957.
(13) Ougizawa, T.; Walsh, D. J.; Dee, G. T., to be published.

Tracer Diffusion of Linear Polystyrenes in Dilute, Semidilute, and Concentrated Poly(vinyl methyl ether) Solutions

L. M. Wheeler† and T. P. Lodge*

Department of Chemistry, University of Minnesota, Minneapolis, Minnesota 55455.
Received October 12, 1988; Revised Manuscript Received February 1, 1989

ABSTRACT: Tracer diffusion coefficients, D, for four linear polystyrenes ($M_w = 6.5 \times 10^4$, 1.79×10^5, 4.22×10^5, and 1.05×10^6) have been measured in solutions of poly(vinyl methyl ether)/*o*-fluorotoluene, as functions of matrix molecular weight ($P_w = 1.4 \times 10^5$, 6.3×10^5, and 1.3×10^6) and matrix concentration ($0 \le c \le 0.30$ g/mL), by dynamic light scattering. The data have been corrected for the concentration dependence of the local friction, using pulsed-field-gradient NMR measurements of solvent diffusivity. The behavior of $D(M,P,c)$ is not consistent with the basic reptation-plus-scaling approach, in that a regime where $D \sim M^{-2}P^0c^{-1.75}$ is not observed. Apparent M exponents vary between −0.56 at very low c and −2.3 at relatively high P and c. A regime where D is independent of P is not established over this range of variables. The c dependence approaches power law behavior at high concentrations, where $D \sim c^{-3.3}$. All the data can be collapsed to a master curve when plotted as D/D_0 versus c/c', where c' is approximated as $(c^*_{PS}c^*_{PVME})^{0.5}$. The data can be interpreted in terms of a gradual transition to diffusion by reptation with increasing concentration, as suggested by more recent theoretical approaches. At the same time, however, it is not possible to eliminate other proposed mechanisms, such as those invoking cooperative chain motion or intermolecular hydrodynamic interactions, solely on the basis of measurements of D for linear polymers. In an accompanying article, measurements of D for 3-arm and 12-arm stars in the same matrix solutions are presented, which lend substantial support to the basic correctness of the reptation picture.

Introduction

The dynamics of polymers in semidilute and concentrated solutions remains a subject of considerable interest, as evidenced by both the number of experimental studies and the variety of theoretical approaches that have been brought to bear. The reptation postulate of de Gennes[1] has provided much of the impetus for recent work in this area, but it is certainly not yet established under what solution conditions reptation becomes the primary mode of polymer motion or even if it is necessary to invoke reptation in describing dynamics in solution. A good deal of attention has been directed toward experimental studies of the translational diffusion coefficient, D, because it is a property that may be defined for a single molecule and because the relevant models can make explicit predictions for the dependence of D on the diffusant molecular weight, M, the matrix molecular weight, P, and the matrix concentration, c.

There is no question that nondilute solutions are very difficult to treat theoretically. Unlike the limit of infinite dilution, where D is influenced primarily by intramolecular hydrodynamic interactions, or polymer melts, where D reflects mainly the mutual uncrossability of neighboring chains, D in solution involves both hydrodynamic and topological contributions. Furthermore, changes in local friction and in effective solvent quality with changing concentration can exert a significant influence on D. One consequence of this complexity is the necessity of making substantial assumptions in theoretical treatments. Another consequence is the danger inherent in extracting power law exponents from data; it is very difficult to vary M, P, or c by an order of magnitude without changing the solution conditions for which a given set of assumptions apply.

Theoretical approaches to the prediction of $D(M,P,c)$ may be classified into four categories. The first is the basic reptation-plus-scaling approach, in which the process of reptation, originally proposed for the motion of an unattached chain in a network, is assumed to apply in semidilute solutions; a straightforward scaling argument leads to the well-known predictions $D \sim M^{-2}c^{-1.75}$ and $D \sim M^{-2}c^{-3}$ for good-solvent and Θ-solvent conditions, respectively.[2] Implicit in this argument is the prediction that D is independent of P when $P \ge M$. The second category includes extensions and revisions of the basic reptation approach. Notable among these is the treatment of Hess,[3,4] who began with a Fokker–Planck equation describing the solution and arrived at the previous predictions as limiting behavior. The crucial assumption in this development is that hard-core repulsive interchain interactions constrain a given chain to move longitudinally. The even more recent model of Kavassalis and Noolandi[5-7] also recovers the reptation predictions in appropriate limits but makes the additional intriguing prediction that the concentration for the onset of entanglement, c_e, is always a factor of 8–10 larger than the overlap concentration, c^*. In contrast, the original scaling arguments do not consider c_e to be distinct from c^*. The third category includes models for which the dominant interaction is still topological, as is the case for reptation, but these interactions are reflected in the cooperative motions of neighboring chains. Somewhat rem-

* Author to whom correspondence should be addressed.
† Current address: Exxon Chemical Americas, Linden Technology Center, Linden, NJ 07036.

0024-9297/89/2222-3399$01.50/0